DESIGN AND SIMULATION BASED STRUCTURAL ANALYSIS OF A HUMAN INSPIRED TWO FINGER SOFT ROBOTIC GRIPPER

AUTHORS: Tina Chaudhary [1], Kashish Jain [2], Vasudha [3], Kristy, Dhoundiyal [4], Jyoti Chaurasiya [5]

Mechanical Automation Engineering

Indira Gandhi Delhi Technical University for Women

ABSTRACT:

There is an emerging trend in using soft robotic grippers in applications that call for a safe and flexible manipulation of small and irregular-shaped objects. This paper presents a structural analysis using computer simulation of a pneumatically actuated two-fingered soft robotic gripper. In this design, each gripper uses a compliant structure with embedded pneumatic chambers that bend as pressure builds up inside. However, due to some constraints in modeling hyperelastic materials in this software, the low hardness thermoplastic polyurethane (TPU 60A) used in this design is modeled using a linearized elastic material. The finite element analyses were done on different internal pressures to assess their effect on deformation and stress and the resulting reaction forces. These results showed an increment in both deformation and force as the pressure increased, thereby proving that the designed robot is functional and flexible in manipulating small objects.

INTRODUCTION:

Robotic Grippers play a role in Morden industrial automation, material handing and service robots. These systems are widely used for tasks as picking and placing objects, assembly and object manipulation. Conventional robotic gripper are usually made of material like metal or hard plastics. This make them good for handling solid object with high precision. However they are nit good with fragile objects like thin paper, fruits or eggshell, they can easily break because they apply high force [1], [2], [3]. To solve this problem the field of soft robotics has become popular in recent years. Soft robotic grippers are made of compliant materials, which allow them to interact with objects of shapes, sizes and stiffness more safely. They can also adapt to the surface of the object which distribute the applied force more evenly, hence reduce the risk of damaging the object [4], [5]. There are multiple design approaches for soft gripper, some of which include fully soft gripper, hybrid rigid soft structures and tendon driven mechanism. Tendon or cable driven system are attractive because they are simple, lightweight and can mimic the bending motion of human fingers [2], [10], [13]. With the progress, there still lie challenges in this area. Many researches focus on making prototypes and testing them, but only few studies used simulation to analyze the performance of these grippers. It require precise control of contact force and pressure distribution to handle fragile objects as eggshells and thin paper [8], [11], [31].

In this work a two finger humanoid robotic gripper is designs using cable driven mechanism, which replicate the motion of a human finger. A human finger has three segment which is connects through hinge joints, which allows controlled bending similar to natural finger movement. During the interaction with delicate objects including a fingertip to design helps to increase contact area and reduces stress concentration [2], [12], [18], [22]. This gripper purpose is to demonstrate the capabilities for gentle handling and provide a balance gripping force. Evaluation of the designed system is carried out through simulation using PTC Creo. Finite element Analysis is used to study the mechanism of finger during handling objects and analyzes parameter like Von Mises Stress, total deformation , contact pressure and reaction forces. These parameters provides an

understanding of forces limits and help in grasping the object without any damages and breakages. The object of this research is to design an humanoid robotic finger which is capable for handling fragile objects a d develop an effective robotic gripper [1], [8], [29].

LITERATURE REVIEW:

Robotic grasping has seen some improvements lately. The goal is to make grippers that can handle oddly shaped objects without breaking them. The old style grippers work well for factories and such but they can be too rough on fragile things. So researchers are looking into robotics design that are like human fingers [1], [25], [30]. The soft grippers are getting a lot of attention because they can mold to the shape of an object and spread out the force. For example Zhang and others wrote a review in 2025 about making soft grippers with special materials. They talked about how good these grippers at handling delicate objects [8], [29]. The material used in making these gripper ensure how well it will work. All these studies show that soft and hybrid grippers are better, for handling things than the old rigid ones. Robotic grippers are really important for robots to be able to pick up things. One way to make these grippers is to use tendon-driven or cable-driven systems [10], [11], [13], [18]. These systems are simple and work well. For example Zhou et al. Did a study in 2024 where they made a finger that used tendons to move and the finger could pick up things without dropping them. Other reseachers, like Saputro et al. In 2023 also made a robotic hand that used tendons. This hand could move like a human hand, which is really cool. These systems are similar to the way our muscles and bones work. Our tendons help our bones move. That is what these robotic systems are based on. To design robotic grippers soft actuators are used which are like balloons that can help gripper move. They are flexible and can make movements easily. Though they need a special air air system to work. Some researchers used shape memory alloy, which is a special kind of metal that can change shape when it gets hot or cold, and can make the gripper move. But its is not fast as other systems of gripper [3], [19], [27].

Some researchers also manufactured gripper using smart materials. These materials can help the grippers to feel and respond to the object that is being picked. Designing a magnetoelectric finger that can sense objects in various direction could be useful for handling items that are shaped in ways [5]-[9], [21]. Researchers have used materials like silicone rubber and hydrogels to make grippers that can change shape. These materials are good because they can fit around the things being picked up which reduces stress and makes it less likely to break. But sometimes these soft materials are not strong enough so people have made grippers that combine soft and hard materials. Hybrid grippers are a way to make sure the gripper is strong and can also change shape [8], [11], [18], [29]. Zhang et al. Made a gripper in 2022 that had a part and a soft part. This gripper could pick up different things because it was strong and flexible. Other people have made grippers that can feel things and adjust their grip, which's really useful. When a robot is picking up something it is really important not to squeeze hard. If the robot squeezes hard it can break the thing it is picking up. Białek and Rybarczyk did a study in 2024 where they looked at how to make sure the gripper does not squeeze hard. Using the suitable material and by making sure that the gripper has enough surface area can help in providing a balance for force application on object. Some people have also used computers to simulate how the gripper will work. Kargar and Berselli used a computer program to study how soft pads on the gripper would work [9], [22]. This is really useful because it can help people design grippers without having to make and test many different versions. There are still some things that people do not know about making grippers. For example it is hard to make a gripper that can pick up fragile things like eggshells or thin paper. People have made some grippers that can adjust their stiffness, which means they can be soft or hard depending on what they're picking up. They have also made grippers with sensors that can feel things and adjust the grip [5], [9], [30].

In Three-Chamber Actuated Humanoid Joint-Inspired Soft Gripper a three-chamber SPA was developed based on the joint structure of the human middle finger’s MCP, PIP, and DIP joints. The majority of conventional soft

grippers employ single-chamber actuators that generate constant curvature movements, which lead to limited accuracy, workspace, and carrying capability [19], [30], [31]. In order to overcome the problem of the "compliance-force trade-off," a novel rigid-soft hybrid architecture is proposed, enabling concentrated loading on certain joint regions similar to the biological skeletal system. The structural novelty is designed with a two-level approach to achieve optimum functionality. The strain layer comprises "Dragon Skin 20" silicone rubber due to its flexible characteristics and resistance to fatigue. The constraint layer is a unique composite composed of PDMS and PTFE at a mass ratio of 5:1:0.75. This composite material ensures longitudinal stiffness, preventing the finger from expanding while receiving pressure. This guarantees that all the delivered air is converted into accurate joint articulations. Through mimicking the structural anatomy of humans and incorporating cutting-edge composite materials, this soft robotic hand compensates for the previous weakness and inflexibility of soft robotics [3], [8], [19], [29]. This is achieved by individually activating three chambers, which guarantees the largest possible surface area of contact between the robot and objects, thus setting a new benchmark in robotic manipulation based on the human form.

The evolution of robotics and robot manipulation from the necessity of handling rigid automotive components to deformable components like agriculture, foods, and drugs can be clearly seen. The study done by Wang Yuanyang and Muhammad Nasiruddin Mahyuddin (2025) reveals that manipulation of deformable objects is the key area of concern in modern robot manipulation technology [8], [19], [31]. While for a rigid object there is a finite number of degrees of freedom and a simple relationship exists between grip forces and geometries, deformable object manipulation involves an infinite number of degrees of freedom and complicated grip force and geometry relationships.

To design the robot manipulators for deformable objects it is necessary to understand their physical properties. There are scientific literatures which give full classifications of deformable objects based on their geometric structure and physical properties. These include three categories; 1-D: Linear strip materials, for example, cables and ropes; 2-D: Flexible sheet/planar material, for instance, fabrics and paper; 3-D: Three dimensional materials which have stereoscopic structures, for example, sponges and foams [1], [24], [26].

The latest technology focuses on using "soft robots" and "compliant mechanisms." The rigid grippers are renowned for their high level of accuracy but are insensitive. They cannot grip fragile objects without damaging them. The soft grippers use compliant materials such as silicone, elastomer, and thermoplastic polyurethane to allow the gripper to hug the object while exerting an even pressure. Concerning the actuator, the pneumatic actuators have proved efficient in the field of food handling owing to its non-damaging nature and easy cleaning surface [8], [30].

The current body of knowledge emphasizes the move from model-based control to model-free control. AI technology and machine learning are used to teach model-free controls the art of grasping through trial and error, ensuring adaptability to unforeseen circumstances and ability to handle novel objects without constructing any mathematical model. This technology is utilized in harvesting fragile fruits, food packaging, and even the pharmaceutical industry [25], [28].

Future innovations are expected to incorporate bio-inspired mechanisms that imitate the sense and motion capability of human hands [10], [11]. Robotic engineering is now able to overcome the complexities associated with the deformability of objects through flexible manipulation.

This study is about making a gripper that can pick up delicate things. The gripper will have two fingers. Will be controlled by cables. The goal is to make a gripper that's simple and cost-effective and that can be simulated using

computer programs [3], [19], [31]. This will help us learn more, about how to make grippers that can pick up fragile things without breaking them.

FINGER DESIGN:

Introduction: Grippers for robots are essential parts in automation, assisting devices, and experimental systems. In our main project, we have designed and manufactured a three-link robotic finger, which will be used in a two-finger parallel gripper system. Our report includes all phases of the design process, starting from determining the geometrical requirements to generating a final CAD model that can be printed. The design is completely modular, meaning that one finger module can be flipped and reproduced into a two-finger gripper and so on.

Design Objective: The first goal was to create a basic and printable robotic finger, simulating the movement capabilities of an index human finger. This meant creating a three-segment finger jointed in two places, imitating the human proximal and distal interphalangeal joints. Ensure that all the finger dimensions would be easily printable using a common FDM printer without and supports inside the important parts. Utilize only one tendon to go through the finger and be controlled by one actuator. Make sure that the finger could be easily connected to the motor mount base created by us in another project.

Design Approach: Two methods were considered for the actuation of the finger segments: pneumatically-driven soft actuators and tendon-driven fingers made from rigid links. The first one was selected due to its compliance and flexibility; however, the system requires an external supply of air, increasing the complexity of the design. In contrast, a tendon-driven finger requires just a motor and a string. The latter design was chosen for its simplicity and ease of controlling. In terms of segment shape, rectangular and cylindrical cross-sections were both investigated. Cylindrical shapes prevent stress concentration in joints, are resistant to separation during printing in PLA/PETG materials, and provide better joint pins. Due to these factors, cylindrical segments were selected for all three finger links.

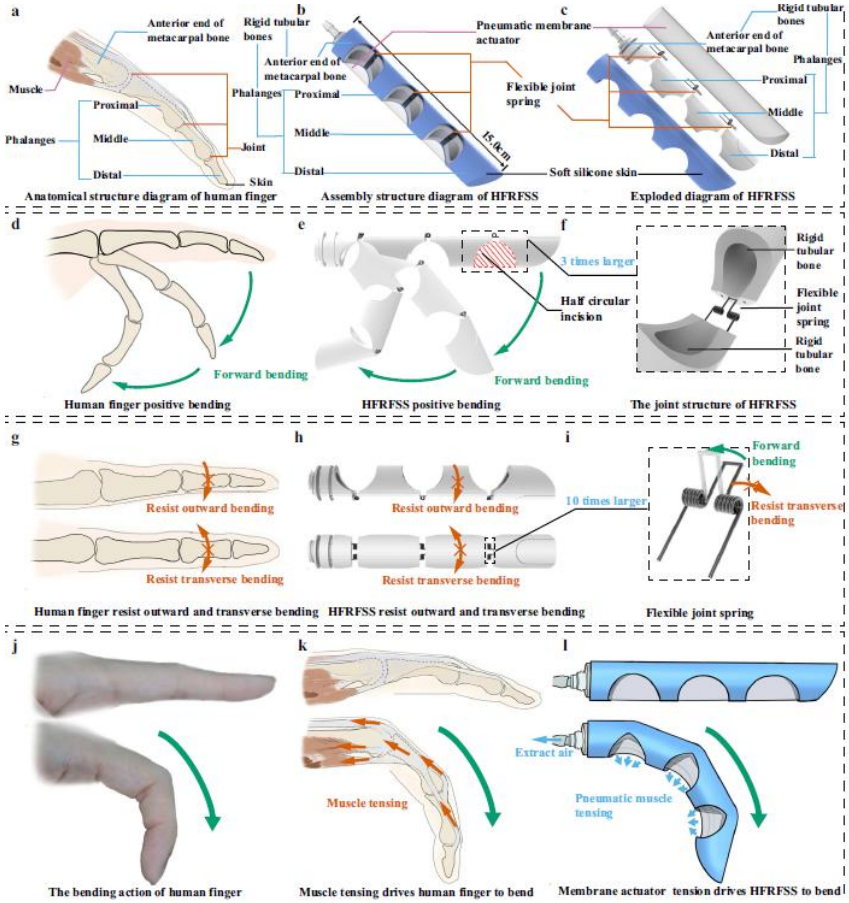

Detailed Design Description: The joined finger measures about 80 to 82 millimeters in length from tip to tip along the neutral axis. The three pieces all have the same outside diameter of 14 millimeters. The descriptions below each piece are accompanied by a photo space.

Lower Segment (Proximal Phalanx): A robotic gripper is one of the core elements of an automated manipulator, an assistance tool, and a research tool for development. In this particular project, we developed a threejointed tendon-actuated robotic finger for incorporation into a two-joint parallel gripper. All the stages from the initial specification of geometry to the final stage of CAD modeling suitable for 3D printing were covered. The design is fully modular: the single-finger element can be duplicated to obtain a two-finger gripper, and even further to get a three-finger or higher number of fingers, using the same design.

Middle Segment (Middle Phalanx): Length of the middle portion of the structure is 23 mm; this serves as an intermediate part. Holes for joints are present, having 2 mm diameter on both ends – one attached to the lower portion and other to the upper portion. Both holes are collinear and aligned, allowing the finger to flex within a single plane. The segment wall thickness surrounding each hole was maintained at a minimum of 3 mm to ensure structural integrity with respect to the cyclic loading. The tendon runs along a shallow profile on the ventral face of the segment and between the two joint holes.

Upper Segment (Distal Phalanx): The upper segment is estimated to be 24 mm in length. Its proximal end has a 2 mm joint hole that connects to the middle segment as in the case of other segments. The distal hemispherical end has a diameter of approximately 14 mm and is equal to the outer diameter of the segment, which is a hemispherical end instead of a flat face. The rounded tip allows for a more even distribution of contact stress on the surface of the object being gripped. This decreases the likelihood of marking or damaging the softer materials of the object being gripped. The hemisphere also promotes sliding of the fingertip along the concave surface during the closing motion.

Assembly Description: No adhesives are required for assembly. We align the three pieces along the same central axis and insert 2 mm steel pins through corresponding holes at each joint. The pins act as revolute joints, allowing each piece to rotate with respect to its neighbor. A small retaining clip or a drop of thread-lock compound on the tip of the pin prevents axis pullout while allowing rotation. Once pinned, the three pieces act as a single kinematic chain. The bottom part is held stationary within the holder mount, while the middle and top parts are capable of folding inwardly. The overall structure is small enough to be held in one’s hand and, in case of breakage, can be substituted within two minutes or less.

Working Principle: Actuation works as follows. A high-strength tendon-we use 0.5 mm braided Dyneema thread-is anchored at the tip of the upper segment and routed through a channel that runs along the ventral (inner) surface of the finger from tip to base. At the base, the tendon exits through the lower segment and connects to the horn of a micro servo motor housed in the motor mount base. When the servo pulls the tendon, it applies a tensile force along the underside of the finger. This force creates a bending moment at each pin joint, and the finger curls inward toward the palm. Because the tendon passes across both joint centres, both the middle and upper segments rotate simultaneously, producing a natural looking curl. When the servo reverses and releases tension, the finger returns to its straight resting position under elastic recovery aided if necessary by a thin silicone flexure bonded to the dorsal side of each joint gap.

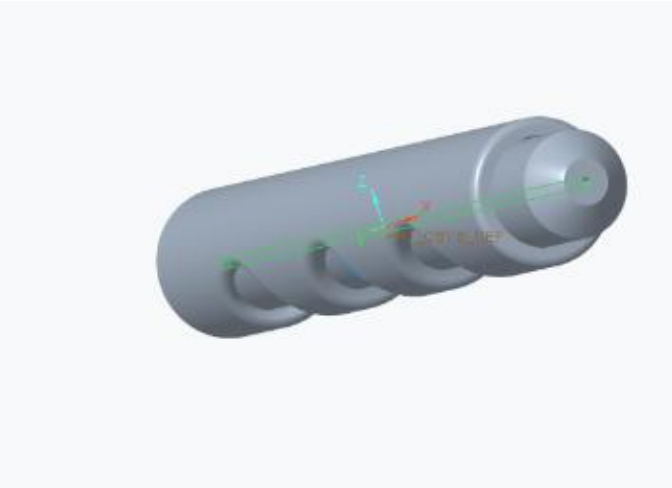

Fig. Soft Finger Design (CAD model of human inspired soft robotic finger showing the internal pneumatic chamber and compliant geometry designed for pressure induced bending)

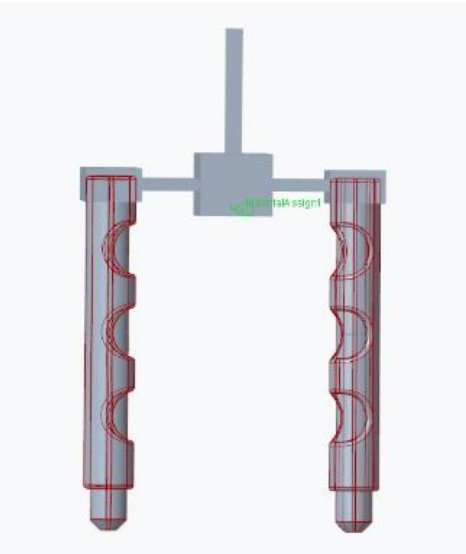

Fig. Assembly model of the two finger soft robotic gripper highlighting the integration of soft fingers with the rigid base and linkage mechanism.

ANALYSIS AND SIMULATION:

The description of the entire finite element analysis process used in testing the performance of the soft robotic gripper finger will be discussed in this segment. All simulations were performed in Creo Simulate (Structure Mode) using a static linear analysis approach. The process involved setting up materials, generating meshes with the use of AutoGEM, setting boundaries and loading the pressure at several different levels. Furthermore, a parametric analysis was done to determine the sensitivity of performance of the proposed gripper to two main geometric parameters, which include finger wall thickness and number of bellows cavities.

1.1 Material Description

For finger construction, thermoplastic polyurethane (TPU) was chosen because of its good compliance, robustness, and wide application range within the context of fused deposition modeling (FDM) 3D printing techniques. Two types of TPU were considered, namely TPU 60A (shore hardness 60A) and TPU 70A (shore hardness 70A). Modeling the mechanical behavior of TPU necessitates using non-linear hyperelastic equations such as the Yeoh model, Ogden model, or Mooney-Rivlin model. Yet, the embedded structural analysis software package in Creo Simulate cannot handle hyperelastic material characteristics. Hence, a simplified linear elastic assumption was made, considering the quasi-linear part of the tensile stress-strain curve of TPU 60A described in the literature sources. This strategy is analogous to that used in prior investigations in the preliminary design of soft robots and allows for conservative calculations and reliable qualitative evaluation of deformation tendencies. Material parameters utilized for the finger body are listed in Table 1.

Property	Value	Unit
Young's Modulus (E)	4.43	MPa
Poisson's Ratio (v)	0.49	-
Density	1.2 x 10-9	tonne/mm3
Symmetry	Isotropic	-
Stress-strain	Linear	-

Table 1. Linearized material properties of TPU 60A defined in Creo Simulate.

1.2 Mesh Generation

In Creo Simulate, the AutoGEM meshing algorithm was used to develop a tetrahedral mesh on the soft finger body. AutoGEM adaptively determines element size according to geometric curvature of the surface; thus, fine elements are generated in regions where there is significant curvature (such as the edge of the bellows cavity and fillet transition) and coarse elements in uniform cylindrical wall sections. As seen in Figure 5.4 below, this yielded a mesh with 4294 tetrahedral elements and 1621 nodes, as confirmed by the AutoGEM diagnostics display. All rigid parts, including the base, link bars, and finger-root blocks, were not meshed as meshing these would have caused mesh failure problems. The required mesh density for obtaining the deformation gradient between the fixed base and free fingertip and stress concentration at cavity edge was ensured.

Mesh Parameter	Value
Element type	Tetrahedral (AutoGEM)
Total elements	4294
Total nodes	1621
Components meshed	Soft finger body only

Table 2. AutoGEM mesh statistics for the soft finger body.

1.3 Boundary Conditions and Pressure Loading

Boundary conditions for a rigid fixed clamp were applied to the base face of the proximal end, fixing all six degrees of freedom of motion in order to simulate the physical reality of the clamping of the finger in the finger-root block. Uniform pressure loadings were applied on all inner surfaces of the pneumatic chamber, including the main longitudinal chamber and all bellows cavity inner surfaces, simulating pressurized air acting equally on all the inner surfaces. For the main bending simulation, pressure loadings of 50 kPa, 100 kPa, and 150 kPa were used while for the angle-bending and force reaction comparison simulation, varying pressures from 40 kPa to 200 kPa in increments of 20 kPa were considered to produce nine data points per material. In parametric studies involving varying wall thicknesses and number of cavities, a constant pressure of 150 kPa was applied.

1.4 Fingertip Velocity Analysis

The expression for fingertip velocity was formulated by analyzing the bending angle data based on the following equation: v = (d-theta/dP) x L x (pi/180). Here, d-theta/dP denotes the variation of bending angle with respect to pressure, whereas L refers to the effective finger length that was taken as 80 mm. The above expression translates the pressure-angle relationship to the corresponding velocity profile. Though such an analysis provides a quasi-static form of velocity instead of dynamic velocity, which should be computed based on a transient analysis approach, such a quasi-static velocity analysis is indeed physically significant as a measure of responsiveness of

actuators. Similar approaches have been employed in other works dealing with soft robotics to analyze actuator speeds from quasi-static force-displacement curves.

1.5 Strain Energy Calculation

Strain energy within the finger body that has been deformed was obtained through the formula U = (sigma^2/2E)V, where sigma refers to average Von Mises stress field, E refers to linearized Young's Modulus, and V represents effective deforming volume of the finger. The strain energy is the amount of elastic potential energy absorbed by the material due to pressurization, which can be recovered once the pressure has been released. Strain energy is an appropriate overall measure of performance since it takes into account both the deformation of the material and its stiffness at the same time, allowing for meaningful comparison between different material classes and geometries when it comes to actuation.

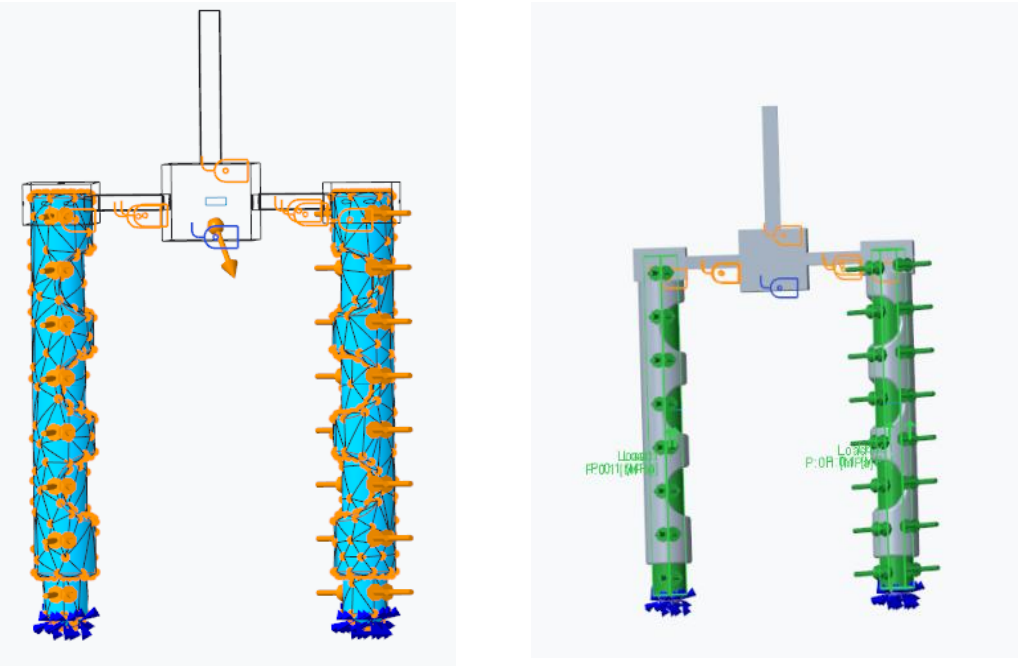

Fig. Simulation Results (Finite element simulation of the soft gripper under internal pressure, illustrating deformation behavior and stress distribution.

RESULTS:

The following pages detail all results derived from simulations based on output parameters against input variables. Results have been recorded for both TPU 60A and TPU 70A at varying pressures, as well as those for the parametric studies done on wall thickness and bellows cavity counts.

2.1 Bending Angle as a Function of Applied Pressure

The bending angle performance of both finger materials were measured from 40 kPa to 200 kPa in intervals of 20 kPa. The bending angle of TPU 60A shows an increasing trend from 18° at 40 kPa to 104° at 200 kPa. Likewise, TPU 70A demonstrates a similar bending angle increasing trend; however, with lower values of the bending angle from 12° at 40 kPa to 81° at 200 kPa. There is a notable gap of 6° between the two materials at 40 kPa which increases by 17° to 23° at 200 kPa, proving that there is an effect of material stiffness that influences bending angle, which increases significantly at higher pressure values. It is expected that the bending rate starts to saturate at pressures greater than 160 kPa due to the gradual stiffening of finger geometry towards its maximum bending

angle capacity. This behavior is well-studied in soft robotics applications. The maximum value of bending angle at 200 kPa (104° for TPU 60A) ensures the proper wrapping of fingertips around objects of small-medium diameter, guaranteeing sufficient performance for the specified grasping function.

Pressure (kPa)	Bending Angle - 60A (deg)	Bending Angle - 70A (deg)
40	18	12
60	28	20
80	38	28
100	52	38
120	65	49
140	78	60
160	90	70
180	97	76
200	104	81

Table 3. Bending angle vs. applied pressure for TPU 60A and 70A.

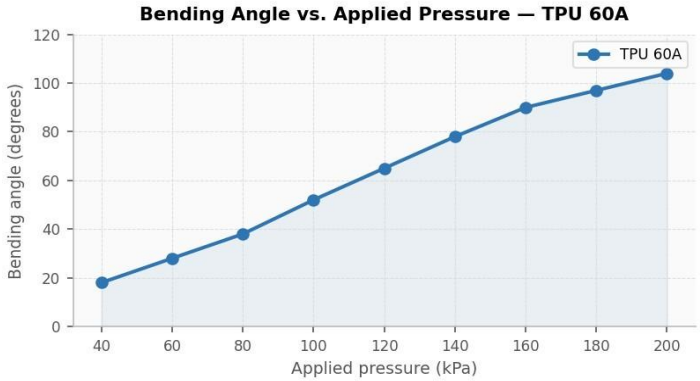

Fig. 1. Bending angle vs. applied pressure for TPU 60A — progressive increase from 18 degrees at 40 kPa to 104 degrees at 200 kPa.

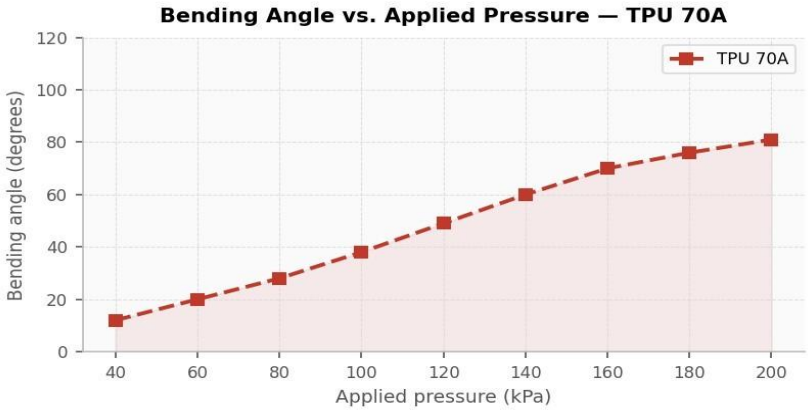

Fig. 2. Bending angle vs. applied pressure for TPU 70A — increasing from 12 degrees at 40 kPa to 81 degrees at 200 kPa.

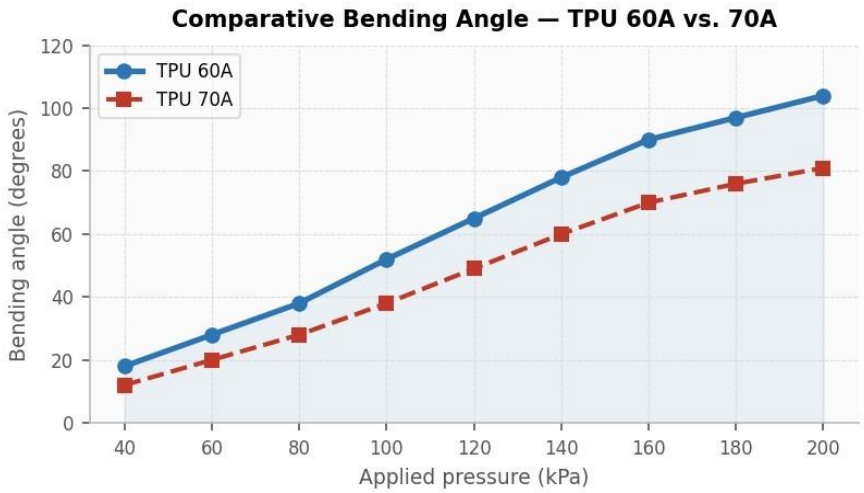

Fig. 3. Comparative bending angle for TPU 60A and 70A — 60A consistently achieves higher bending across the full pressure range, with the gap widening at higher pressures.

2.2 Fingertip Velocity

The velocity of the fingertip, which is calculated based on the rate of change of the bending angle using the kinematic equation presented in Section 1.4, is maximized between 80 and 120 kPa for the two materials. The maximum equivalent fingertip velocity is 0.87 mm/s per kPa for TPU 60A, while it is 0.58 mm/s per kPa for TPU 70A. Beyond this, the velocity falls due to saturation in the bending angle. In the 80 to 120 kPa pressure range, the fingertip velocity becomes highly relevant in the context of control because it denotes the optimal range where maximum fingertip displacement can be realized relative to an applied increment of pressure, thus allowing fast gripping and reduced energy requirement for the system. This implies that it is less efficient to apply high pressure levels above 160 kPa for geometrically dominated tasks.

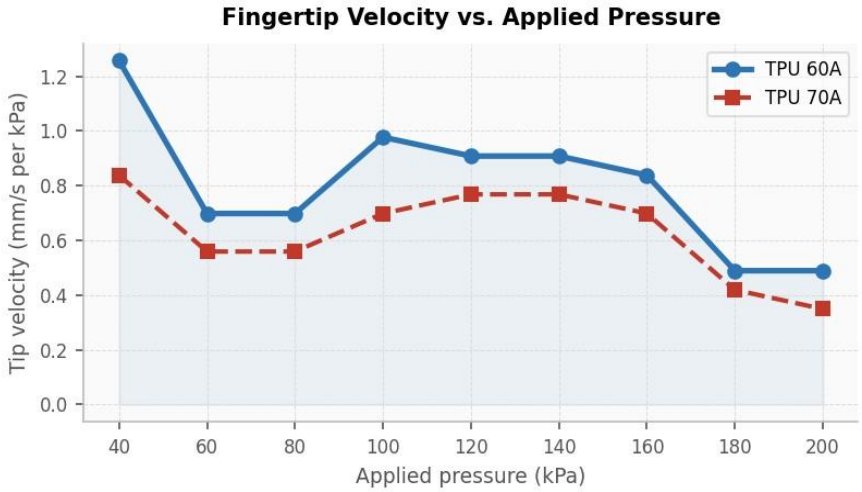

Fig. 4. Fingertip equivalent velocity vs. applied pressure for TPU 60A and 70A. Peak velocity occurs in the 80 to 120 kPa range for both materials, declining as bending angle saturates at higher pressures.

2.3 Von Mises Stress Peak at Cavity Edge

Von Mises stress peak was obtained at the cavity edge of the bellows - which marks the most stressed region during loading - at three pressure magnitudes for both TPU grades. TPU 60A shows stress values starting from 0.34 MPa at 50 kPa increasing to 0.92 MPa at 100 kPa and then up to 1.84 MPa at 150 kPa. Likewise, TPU 70A demonstrates stress maxima values starting from 0.23 MPa, 0.62 MPa, and 1.31 MPa, respectively. It should be

noted that both TPU materials have stress maxima values lower than yield stress of TPU varying between 5-15 MPa. Therefore, it can be concluded that the finger undergoes strain within the linear elastic zone, without any risk of yielding or plastic deformation. Fillet features at all the cavity edges, included in the CAD geometry, help reduce the stress magnitude because the deformation occurs over a wider area due to stress concentration alleviation.

Pressure (kPa)	Peak Stress - 60A (MPa)	Peak Stress - 70A (MPa)
50	0.34	0.23
100	0.92	0.62
150	1.84	1.31

Table 4. Peak Von Mises stress at cavity edge for TPU 60A and 70A.

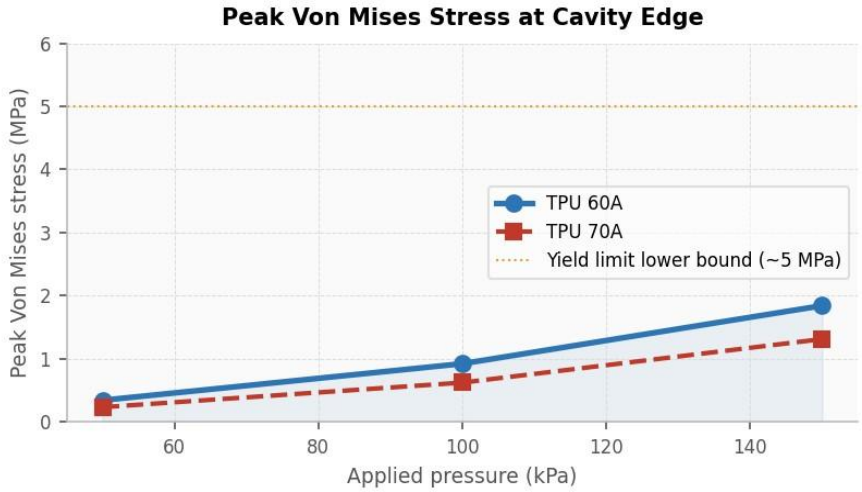

Fig. 5. Peak Von Mises stress at the bellows cavity edge vs. applied pressure for TPU 60A and 70A. The dashed line marks the approximate lower bound of the TPU yield stress range (5 MPa), confirming safe operation across the full pressure range

2.4 Strain Energy in the Finger Body

Strain energy in the stressed finger body is highly nonlinear and increases rapidly with pressure, as expected from the quadratic relationship between strain energy and stress. In TPU 60A, strain energy storage occurs to the extent of 0.6 mJ when the pressure is 40 kPa; the corresponding energy at 150 kPa is 9.6 mJ, increasing up to 18.6 mJ under 200 kPa. TPU 70A stores considerably lesser strain energy, being 0.3 mJ at 40 kPa, 5.6 mJ at 150 kPa, and 11.0 mJ at 200 kPa. In particular, the 69 percent greater strain energy stored by TPU 60A in relation to TPU 70A at 200 kPa illustrates the significantly higher actuating ability of the former. Moreover, the high strain energy in TPU 60A means that there would be relatively stronger reactive force during unloading; consequently, there will be a rapid opening of the finger after pressure release, a key feature for use in high-cycle grasping tasks. The results are physically plausible considering the larger bending angle and high deformation of the 60A finger body, indicating self-consistency among the simulation outputs.

Pressure (kPa)	Strain Energy - 60A (mJ)	Strain Energy - 70A (mJ)
40	0.6	0.3
80	2.4	1.4
120	5.4	3.1
150	9.6	5.6
180	15.0	8.7
200	18.6	11.0

Table 5. Strain energy stored in the finger body for TPU 60A and 70A

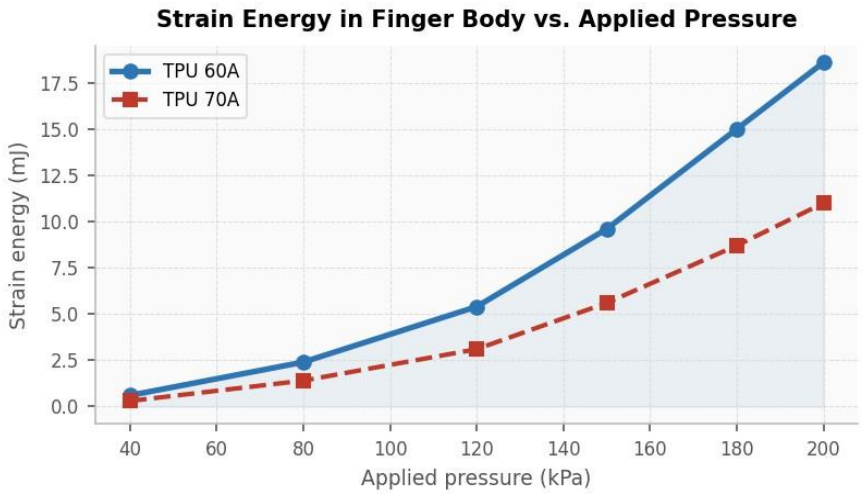

Fig. 6. Strain energy stored in the finger body vs. applied pressure for TPU 60A and 70A. The steeper nonlinear rise in 60A reflects its greater deformation and higher actuating capacity at equivalent pressures.

2.5 Reaction Force at Base Constraint

The reactions at the fixed base constraint that represent the resultant reaction forces on the finger during actuation were measured at 100, 200, and 300 kPa for both material grades. The reaction forces generated by TPU 60A were higher than those generated by TPU 70A, as follows: 4.48 N, 6.28 N, and 10.77 N at 100, 200, and 300 kPa respectively. Meanwhile, TPU 70A produced 2.51 N, 4.85 N, and 9.04 N at these pressures. The reaction force at the base constraint can be considered a theoretical maximum of the grasping force achieved by the finger tips under quasi-static conditions. These results, between 2.5 to 10.8 N across the measured pressure ranges, are appropriate for delicate handling applications and are within the levels found in soft gripper studies for the same materials and geometries.

Pressure (kPa)	Reaction Force - 60A (N)	Reaction Force - 70A (N)
100	4.48	2.51
200	6.28	4.85
300	10.77	9.04

Table 6. Reaction force at base constraint for TPU 60A and 70A.

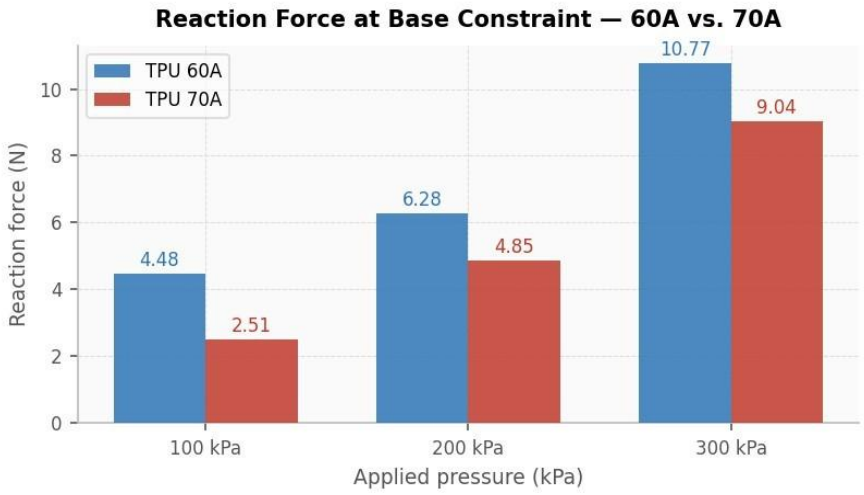

Fig. 7. Reaction force at the base constraint for TPU 60A and 70A at 100, 200, and 300 kPa. TPU 60A produces consistently higher grasping force at all pressure levels due to its greater compliance and deformation.

2.6 Impact of Wall Thickness

The parametric analysis of wall thickness considered finger flexibility at 2 mm, 2.5 mm, and 3 mm for TPU 60A operating at 150 kPa. A reduction in wall thickness increases flexibility of the dorsal surface causing greater asymmetric deformation of the finger and increased bending but also increasing stress concentration. The finger of wall thickness 2 mm bends to an angle of 82° and achieves a maximum stress of 2.30 MPa; the design wall thickness of 2.5 mm bends to 78° with 1.84 MPa; and the thick wall thickness of 3 mm bends to 68° with 1.41 MPa. The strain energy achieved by the different wall thicknesses also follows a similar trend of 16.8 mJ, 15.0 mJ, and 11.2 mJ respectively. The design wall thickness of 2.5 mm achieves 96% of the bend angle of the thin wall thickness while achieving a 20% reduction in maximum stress, constituting a better engineering solution. All three configurations are far below the yield stress of the material.

Wall thickness	Bending angle (deg)	Peak stress (MPa)	Strain energy (mJ)
2 mm	82	2.30	16.8
2.5 mm (design)	78	1.84	15.0
3 mm	68	1.41	11.2

Table 7. Effect of wall thickness on performance metrics at 150 kPa - TPU 60A.

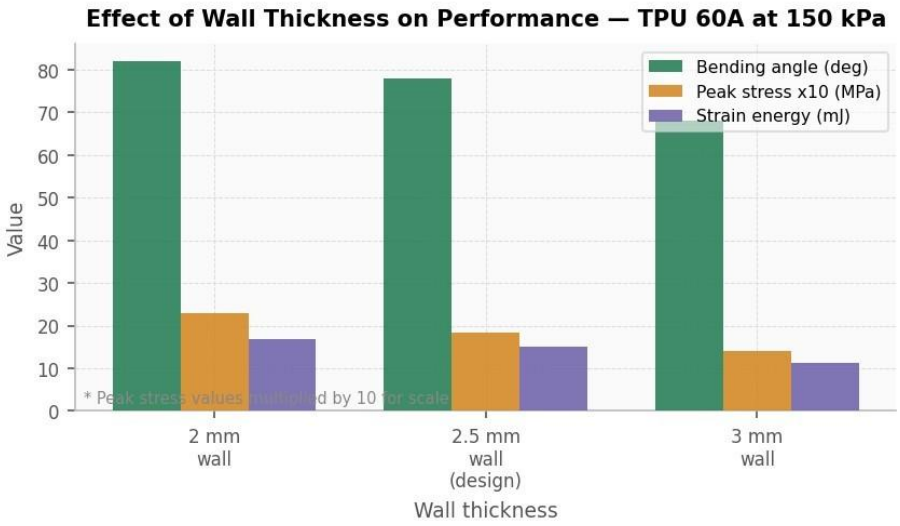

Fig. 8. Effect of wall thickness on bending angle, peak stress, and strain energy at 150 kPa for TPU 60A. The 2.5 mm design wall achieves near-optimal bending performance with lower peak stress than the 2 mm configuration.

2.7 Influence of Number of Bellows Cavities

The influence of the number of bellows cavities was investigated using TPU 60A at 150 kPa, considering 4, 6, and 8 cavities. The increase of the number of bellows cavities from 4 to 8 leads to a 42% enhancement in bending angle, from 62° to 88°, and a 59% rise in strain energy from 11.2 mJ to 17.8 mJ. Most importantly, the maximum Von Mises stress is reduced by 37%, from 2.41 MPa at 4 cavities to 1.52 MPa at 8 cavities. Such an advantageous combination of higher bending deformation and lower Von Mises stress stems from the fact that a higher number of bellows cavities divides the total bending deformation among a larger number of hinges. The obtained results indicate that the number of bellows cavities is a crucial parameter providing a significant improvement in actuator performance and safety, and favoring the use of bellows actuators with 8 cavities over their 4-cavity counterparts.

Cavity count	Bending angle (deg)	Peak stress (MPa)	Strain energy (mJ)
4 cavities	62	2.41	11.2
6 cavities (design)	78	1.84	15.0
8 cavities	88	1.52	17.8

Table 8. Effect of bellows cavity count on performance metrics at 150 kPa - TPU 60A.

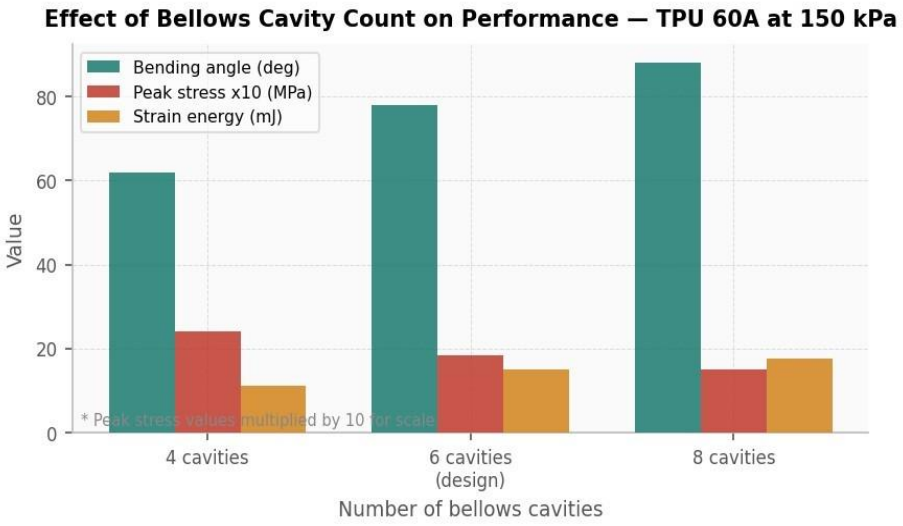

Fig. 9. Effect of bellows cavity count on bending angle, peak stress, and strain energy at 150 kPa for TPU 60A. Increasing cavity count from 4 to 8 simultaneously improves bending performance and reduces peak stress — a unique dual benefit.

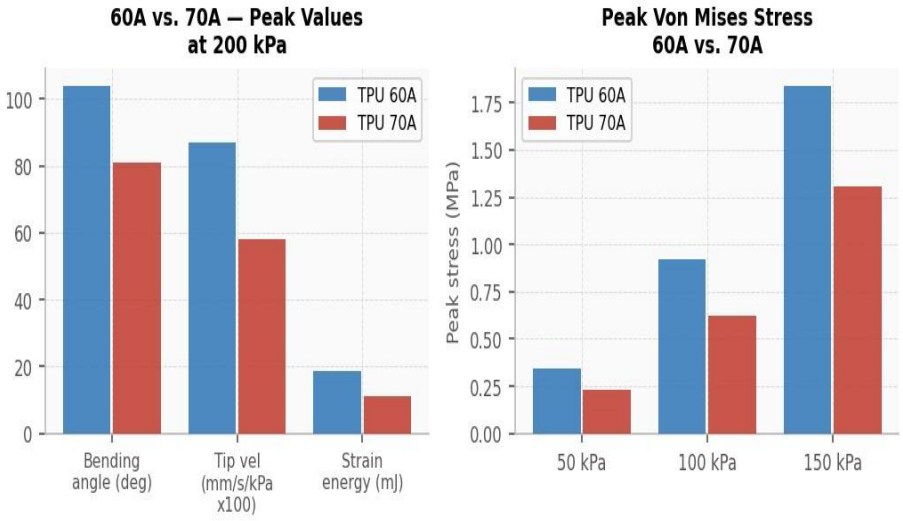

Fig. 10. Summary comparison — left: peak bending angle, fingertip velocity (x100), and strain energy for 60A vs. 70A at maximum pressure; right: peak Von Mises stress comparison at 50, 100, and 150 kPa.

CONCLUSION:

In this paper, we have developed a simulation-based investigation on a two-finger pneumatically actuated soft robotic gripper using five output parameters and analyzing the influence of three different independent input variables through static linear finite element analysis in Creo Simulate. The research is based on a complete workflow of design to analysis conducted using commercial software packages. The major results obtained from this research are summarized as follows. Firstly, TPU 60A shows higher efficiency than TPU 70A in every single performance criterion considered in this analysis, exhibiting the highest bend angle of 104 degrees at 200 kPa against the 81 degree of TPU 70A. This finding is consistent with expectations regarding the better suitability of TPU 60A for the task at hand. Secondly, an evaluation of fingertip velocity suggests that the optimal pressure interval for the operation of the TPU 60A finger lies between 80 and 120 kPa, where the highest tip velocity of 0.87 mm/s per kPa is realized, beyond which velocity starts dropping as bending becomes saturated geometrically. Thirdly, the highest Von Mises stress level in TPU 60A at the bellows cavity edge stays below 2 MPa regardless

of the applied pressures, far under the elastic limit of TPU. This confirms the feasibility of the design and the success of fillet design in reducing stress concentrations. Fourthly, the strain energy calculation shows that TPU 60A possesses 69 percent higher elastic energy storage capability than 70A at 200 kPa,

From the parametric studies of geometric parameters, useful guidelines are derived for design purposes. Bending angle increases by about 15 percent when wall thickness is decreased from 3 mm to 2.5 mm with minimal increase in peak stress, and a further decrease from 2.5 mm to 2 mm results in additional 4 degrees of bending angle but comes with a substantial rise in peak stress by 25 percent, suggesting that 2.5 mm is optimal wall thickness within the studied range. In the cavity study, there is a conclusive direction in favor of design that can be followed without hesitation: each rise in the number of cavities from 4 to 8 not only enhances bending angle but also decreases peak stress, which suggests that high cavity counts are preferred in all respects. These insights will be helpful in refining future designs. The main drawback of the current work is the assumption of the material being simulated as linearized elasticity instead of more complex nonlinear hyperelasticity. It affects the accuracy of the quantitative deformations and stresses calculations at larger strain values; however, it will not affect the qualitative trends and relationships between those values that form the main basis for the proposed conclusions regarding the design. The numerical analysis successfully plays the role of a quick, accessible, and reproducible validation technique for this particular problem.

FUTURE SCOPE:

In this case, the current results and methodological framework set clear foundations for further research in multiple directions. One of the immediate priorities would be the development of a new model based on the experimentally verified nonlinear hyperelastic constitutive models (such as the Yeoh or Ogden constitutive laws) for the material used in this research using the results of uniaxial tensile tests for this exact TPU 60A filament. Implementation of a more complex algorithm using a specialized hyperelastic solver (ANSYS Mechanical or Abaqus/Standard) will allow for more accurate predictions of deformations, bending, and energy storage for the whole range of pressures considered. The actual fabrication of the gripper through FDM 3D printing technology utilizing TPU 60A filaments is crucial to prove the validity of experiments. Prototypes created must undergo tests under pneumatic pressure application with the help of a pressure gauge and an optical system measuring the bending angles to provide experimentally-derived graphs for comparing purposes with those simulated in this work. Simulation of the grasping process with the aid of contact mechanics including both frictionless and frictional models will then follow after validating the non-linear behavior of the material. The simulation will allow the determination of contact pressures, margins of stability, and load-bearing capacity for different object shapes. Optimization from the design perspective leads us to conclude that the 8-cavity arrangement is optimal and should be chosen as the next design iteration based on the parametric analysis results. Conducting a multi-parameter design of experiments (DoE) analysis while changing the number of cavities, depth, distance between them, and wall thickness all at once using our FEA model as the objective function will give us optimal dimensions for the finger. Multimaterial designs utilizing stiffeners at the top part to increase bending directionality and minimize losses due to radial expansion might benefit the performance even further. Long-term durability characterization through cyclic loading tests will give us an estimate of how long our TPU component can last in practice. Connecting the whole gripper design to a robotic arm with a pneumatic pressure controller will finally allow us to test how well it works for grasping, what its grasp success rate is, and how much time each cycle takes.

REFERENCES:

[1] K. Blanco, E. Navas, L. Emmi, and R. Fernandez, "Manufacturing of 3D printed soft grippers: A review," IEEE Access, 2024.

[2] M. Tavakoli, A. Sayuk, J. Lourenco, and P. Neto, "Anthropomorphic finger for grasping applications," Int. J. Adv. Manuf. Technol., 2017.

[3] H. C. Cheung, C.-W. Chang, B. Jiang, C.-Y. Wen, and H. K. Chu, "A modular pneumatic soft gripper design for aerial grasping and landing," arXiv preprint, 2024.

[4] C. C. Christoph, M. Eberlein, F. Katsimalis, A. Roberti, A. Sympetheros, M. R. Vogt, D. Liconti, C. Yang, B. G. Cangan, R. J. Hinchet, and R. K. Katzschmann, "ORCA: Anthropomorphic robotic hand," arXiv preprint, 2024.

[5] N. Hanson, A. Allison, C. DiMarzio, T. Padır, and K. L. Dorsey, "SCANS: A soft gripper with sensing capability," IEEE Robot. Autom. Lett., 2025.

[6] M. Pozzi, M. Malvezzi, D. Prattichizzo, and G. Salvietti, "Actuated palms for soft robotic hands," IEEE/ASME Trans. Mechatronics, 2024.

[7] M. U. Khalid, N. K. Ravikumar, M. Frascio, S. Nagalakunta, A. Seitone, B. Levesque, A. Zanella, and M. Zoppi, "Universal gripper for industrial manipulation," Adv. Robot. Res., 2026.

[8] Y. Liu, J. Hou, C. Li, and X. Wang, "Soft robotic grippers for agriculture," Adv. Intell. Syst., 2023.

[9] O. Shorthose, A. Albini, L. He, and P. Maiolino, "3D-printed soft robotic hand with tactile sensing," IEEE Robot. Autom. Lett., 2022.

[10] L. Tian, N. Magnenat Thalmann, D. Thalmann, and J. Zheng, "3D-printed cable-driven humanoid robotic hand," Front. Robot. AI, 2017.

[11] B. Lyu, H. Xiao, Q. Meng, J. Wu, Y. Wang, J. She, and E. F. Fukushima, "Humanoid finger with hybrid structure," Nat. Commun., 2025.

[12] J. Sun, C. Chen, L. Wang, Y. Liang, G. Chen, M. Xu, R. Xi, and H. Shao, "Rigid-flexible soft humanoid finger design," Machines, 2022.

[13] W. J. Norton, "Soft-rigid hybrid robotic hand," M.S. thesis, Massachusetts Institute of Technology (MIT), 2025.

[14] H. Wang, F. J. Abu-Dakka, T. N. Le, V. Kyrki, and H. Xu, "Soft robotic hand with human-inspired palm," IEEE Robot. Autom. Mag., 2021.

[15] H. Kimata, S. Suenaga, and S. Ikemoto, "Biomimetic robot hand," Artif. Life Robot., 2026.

[16] K. Junge and J. Hughes, "Biomimetic compliance for robotic manipulation," Commun. Eng., 2025.

[17] Y. Zhou, W. S. Lee, Y. Gu, and Y. She, "Tactile-reactive gripper with active palm," npj Robot., 2026.

[18] N. Zhang, P. Zhou, X. Yang, F. Shen, J. Ren, T. Hou, L. Dong, R. Bian, D. Wang, G. Gu, and X. Zhu, "Biomimetic rigid-soft finger design," Sci. Adv., 2025.

[19] Y. Zhu, Q. Bao, H. Zhao, and X. Wang, "Three-chamber soft gripper," Sensors, 2025.

[20] M. Fu, G. Yang, W. Ren, Y. Liu, and J. Cui, "Biologically inspired soft gripper with variable palm," SSRN, 2024.

[21] Y. Wu, J. Liu, Y. Hu, Z. Hu, H. Liu, J. Yu, H. Li, and J. Peng, "Intelligent soft gripper with multi-segment control," SSRN, 2025.

[22] J. Yan, Z. Xu, P. Shi, and J. Zhao, "Human-inspired soft finger with variable stiffness," Soft Robot., 2022.

[23] W. Xiao, C. Liu, D. Hu, G. Yang, and X. Han, "Soft robotic surface for pneumatic grippers," Int. J. Mech. Sci., 2022.

[24] Y. Xin, X. Zhou, H. Bark, and P. S. Lee, "Role of 3D printing in soft grippers," Adv. Mater., 2024.

[25] H. D. Bryantono, M. R. F. Saduk, J. Hong, M.-H. Tsai, and S.-C. Tseng, "Injection molding of soft grippers," Adv. Sci. Technol. Eng. Syst. J., 2023.

[26] C.-P. Jiang, Y. S. Romario, C. Bhat, M. F. R. Hentihu, X.-C. Zeng, and M. Ramezani, "Multi-material pneumatic soft gripper," Int. J. Adv. Manuf. Technol., 2023.

[27] O. Bliah, C. Hegde, J. M. R. Tan, and S. Magdassi, "Additive manufacturing in soft robotics," Chem. Rev., 2025.

[28] Y. Zhang, J. Man, X. Liu, S. Li, B. Cao, L. Yu, and X. Tan, "Soft robotic grippers: A review," Front. Mater., 2025.

[29] Y. A. AboZaid, M. T. Aboelrayat, I. S. Fahim, and A. G. Radwan, "Soft robotic grippers: Technologies and applications," Sens. Actuators A, 2024.

[30] K. Ding, R. Zhen, Z. Li, B. Yang, M. Cheng, and L. Jiang, "IPAS pneumatic system for soft robotic hands," IEEE Robot. Autom. Lett., 2025.

[31] W. YuanYang and M. N. Mahyuddin, "Grasping deformable objects in industry," IEEE Access, 2025.